# Surface Charges and Calcium Ion Binding of Disk Membrane Vesicles†

Toshiaki Kitano,‡ Taihyun Chang, G. B. Caflisch,§ D. M. Piatt,‖ and Hyuk Yu*

ABSTRACT: Disk membrane vesicles (DMV), prepared by isolating retinal disks of the rod outer segment of bovine retina osmotically swollen in hypotonic media, are examined for their surface charge characteristics and calcium ion binding. The surface charges are deduced by two different methods; one method is through the electrophoretic mobility determined by the technique of electrophoretic light scattering, and the other is through the titration valency obtained by the potentiometric titration. Upon confirming the spherical shape of DMV and determining its radius by elastic and quasi-elastic light scatterings, we arrive at the surface densities of electrokinetic valency and titration valency from the first and second methods, respectively. At pH 7 in 2 mM ionic strength, the electrokinetic and titration valencies are found to be $8 \times 10^4$ per DMV and $1 \times 10^6$ per DMV, respectively, indicating that about 7.5–15% of the total titratable groups are electrokinetically active. In terms of the customary unit of surface charge density, the electrokinetic charge is expressed as 0.47 $\mu C/cm^2$; otherwise, the reciprocal surface charge densities are represented as 3400 $Å^2$/electrokinetic valency and 250–500 $Å^2$/titration valency. The pH dependences of electrophoretic mobility and the translational diffusion coefficient give rise to the isoelectric point of DMV at pH 4.3. Calcium ion binding onto the exterior surface of DMV is probed by measuring the mobility in 2 mM ionic strength at pH 7 as a function of the free calcium ion concentration in the suspending medium, controlled by calcium ion buffers. The observed mobility profile with respect to the calcium concentration is shown to be completely independent of the photochemical state of photopigments on DMV; namely, the unbleached and bleached states have the same calcium ion binding isotherm. Further, the binding can be analyzed by a model of two independent and noncooperative binding sites whereby the high-affinity binding has $1.4 \times 10^4$ sites/DMV with the association constant $K_1 = 4.5 \times 10^4$ $M^{-1}$ at 20 °C and the low-affinity binding has $8 \times 10^3$ sites/DMV and $K_2 = 4 \times 10^2$ $M^{-1}$ at 20 °C. The physiological significance of this work is the observed absence of photosensitivity of $Ca^{2+}$ binding on the DMV surface.

The primary process of vertebrate visual transduction is the photoisomerization of 11-*cis*-retinal of rhodopsin on the disk membranes of the rod outer segment (ROS)[1] of retinal rod cells (Wald, 1968). It has been suggested that there must be an internal neurotransmitter which mediates the photoactivated rhodopsin and the attenuation of sodium current through the plasma membrane of ROS (Baylor & Fourtes, 1970). Yoshikami & Hagins (1971) (Hagins, 1972; Hagins & Yoshikami, 1974) put forth a hypothesis that calcium ion acts as the transmitter which effluxes from the ROS disk membranes upon photoreception and diffuses to the plasma membranes to reduce the sodium dark current. Montal et al. (1977) have expounded on this theme by suggesting that the photoactivated rhodopsin molecules cooperatively form calcium ion channels on the disk membranes. The calcium transmitter hypothesis, commonly known as Hagins' model, has had several of its essential elements examined. First of all, it has been established that there exists a sufficient quantity of calcium within ROS (Liebman, 1974; Szuts & Cone, 1977), consistent with its role as the transmitter. Second, whether a sufficient amount of calcium is photoreleased at an appropriate rate has been addressed by Smith et al. (1977), Szuts & Cone (1977), and Smith & Bauer (1979). Third, whether the photorelease of calcium ion is indeed through the permeability change of disk membranes has been examined by Smith et al. (1977), Smith & Bauer (1979), Kaupp et al. (1979, 1981), and Tyminski et al. (1982). Through these efforts, substantial doubt has been cast on the exactitude of Hagins' model. It now appears as though we cannot even be sure of the location of the photoreleasable calcium pool in ROS, either in the intradiskal space as the model proposes or in the cytoplasm (Szuts, 1980). A test of the photoinduced permeability change of the native disks toward $Ca^{2+}$ in the cytoplasmic milieu is yet to be effected despite several confirmations of the permeability change with reconstituted rhodopsin–phospholipid membrane vesicles (O'Brien et al., 1977; O'Brien, 1979; Tyminski et al., 1982). Among a few alternative proposals that attempt to modify Hagins' model in view of these findings, one can cite a proposal that photoreleased $Ca^{2+}$ of ROS is not required to efflux from the intradiskal space to the cytoplasm but could be derived from the bound $Ca^{2+}$ either on the extradiskal surface (Hemminki, 1975) or on the intradiskal surface (Kaupp et al., 1979).

With such a proposal in mind, this study was undertaken to examine the electrostatic and electrokinetic charges of swollen disk membrane vesicles (DMV) and their $Ca^{2+}$ binding characteristics, particularly relative to a possible change with respect to the photochemical state. For this purpose, we isolate the disks from ROS, swell them into spherical vesicles, and suspend them in well-defined hypotonic media, and their size and shape are determined by light scattering before the charge characteristics are probed (Yu, 1982). It should be noted that there is a clear trade-off between an approximation to native cytoplasm and a well-defined disk system separated from other organelles of ROS. While our suspending medium hardly approximates cytoplasm, we are certain of the disk shape, size, and sidedness of $Ca^{2+}$ binding. In order to confirm whether the binding is on the cytoplasmic side of isolated disks, we

† From the Department of Chemistry, University of Wisconsin, Madison, Wisconsin 53706. *Received January 3, 1983.* Supported by National Institutes of Health Grant EY01483.

‡ On leave from the School of Materials Science, Toyohashi University of Technology, Toyohashi 440, Japan.

§ Present address: Research Laboratories, Eastman Organic Division, Eastman Kodak Co., Kingsport, TN 37662.

‖ Present address: Ivorydale Technical Center, Procter and Gamble Co., Cincinnati, OH 45217.

[1] Abbreviations: ROS, rod outer segment(s); EGTA, ethylene glycol bis(β-aminoethyl ether)-*N,N,N',N'*-tetraacetic acid; DMV, disk membrane vesicle(s); Im, imidazole; BSA, bovine serum albumin.

0006-2960/83/0422-4019$01.50/0 

examined electrophoretic mobility of swollen DMV with the native sidedness intact (Amis et al., 1981a). Since the technique is solely responsive to the surface charge of the electrokinetic units in question, namely, the single bilayered vesicles formed from the disks, there is little ambiguity as to the binding side as long as the disks retain the same sidedness in the vesicular form. It simply probes the exterior surface charge regardless of possible concurrent ion transport into the vesicle interior. We also note that DMV used here are now reasonably well characterized relative to their photopigment content, hypotonic size, and osmotic behaviors, and they can be prepared reproducibly (Smith & Litman, 1982).

There are several constraints in designing the experiment. First, we must reduce the ionic strength of the suspending medium to the millimolar range in order that the disks remain swollen into spherical vesicles; otherwise, the mobility results are not amenable to clean-cut interpretations. Second, the suspensions must be dilute enough that there is negligible interparticle electrokinetic interference among the vesicles. Third, the total ionic strength of the medium must be known precisely while the free $Ca^{2+}$ concentration is changed; thus, the Debye screening length as it affects the mobility must be properly accounted for in order to extract the electrokinetic charge from the observed mobility. The first and third constraints limit the accessible range of $Ca^{2+}$ concentration while the second rules out any conventional optical method to monitor the mobility. In addition, the method should not perturb the photochemical state of the photopigment so that one can probe whether there exists a light-induced mobility change.

Taking these constraints into account, we have chosen the technique of electrophoretic light scattering as most appropriate. It is based on the Doppler shift frequency measurement of laser light scattered by charged particles executing field-induced viscous drift. Since its first development by Ware & Flygare (1971), the technique has undergone substantial refinements (Bennett & Uzgiris, 1973; Uzgiris, 1974; Uzgiris & Kaplan, 1974; Josefowicz & Hallet, 1975; Haas & Ware, 1976; Mohan et al., 1976). We have calibrated our light-scattering instrument (Shaya et al., 1974) with the use of a sample of monomeric bovine serum albumin as the standard (Caflisch et al., 1980).

In this report, we first show the characterization of surface electrostatics of DMV with respect to pH by titration valency and electrokinetic charge and then deduce the binding isotherm of $Ca^{2+}$ on the DMV surface from the profile of electrophoretic mobility over 3.5 logarithmic decades of calcium concentration. Finally, we examine the effect of the photochemical state of rhodopsin on the binding isotherm.

## Materials and Methods

*Materials.* Dark-adapted frozen bovine retinas were obtained from American Stores Packing Co. (Lincoln, NE). The isolation and preparation procedures of the disk membrane vesicles (DMV) follow the method of Smith et al. (1975) with a slight modification (Norisuye et al., 1976; Amis et al., 1981b). Removal of endogenous ions (presumably bound on the extradiskal surface) and free ions is effected in two ways: (1) DMV suspended in deionized water (15-MΩ specific resistivity) are passed through a mixed bed of ion-exchange resins (AG501-X8, Bio-Rad, Richmond, CA), and (2) DMV are washed with 100 μM EGTA before the final suspension is made. Both ways produce the same results insofar as the mobility in the $Ca^{2+}$ free state is concerned (see below). When the first method is unsuccessful, we often obtain an indication of collapsed DMV which can be detected by elastic light scattering. We have usually performed the scattering test to ensure intactness of DMV after the ion-exchange operation.

There are two kinds of suspending media employed here, 2 mM NaCl and 4 mM imidazole (Im) buffer containing 100 or 20 μM EGTA, and their pHs are adjusted with HCl or NaOH solution. The free calcium ion concentration ($C$) is adjusted by adding appropriate amounts of $CaCl_2$ solution to the Im buffer solution; the ionic strength ($I$) and $C$ are calculated by using the dissociation constants of Im and EGTA and the association constants of $Ca^{2+}$ to EGTA given in the literature (Potter & Gergely, 1975). All suspending media were bubbled extensively with argon before use for the purpose of removing dissolved oxygen.

The concentrations of DMV suspensions were determined by measuring the turbidity at 633 nm (Amis et al., 1981a). For the scattering measurements, the DMV number density was usually of the order of $10^9$ vesicles/mL while for the potentiometric titrations it was greater by a factor of $10^2$. The suspensions for the light-scattering measurements were filtered through a 2-μm filter (Nucleopore) directly into the scattering cell. The pH of each scattering suspension was measured before and after the experiment and confirmed to remain the same within 0.1 pH unit. A total of some 40 separate and independent ROS disk preparations were used in this study. All data for a given suspension were collected within 5 h after its preparation in a cold darkroom (4 °C). For bleached samples, the final suspensions prior to the scattering were exposed to light.

*Elastic and Quasi-elastic Light Scattering.* Both of these measurements were performed in order to characterize DMV size and shape as well as the translational diffusion coefficient. The instruments used for elastic light scattering have been built in this laboratory, and an earlier description has appeared elsewhere (Amis et al., 1981a). More recently, we have included the feature of a microcomputer-controlled goniometer; the scattered intensity in the analogue signal is digitized and accumulated 256 times before the goniometer is moved to the next scattering angle, and the scattering angle is incremented by 2°. For the quasi-elastic light-scattering measurements, the instrument used is the same one described elsewhere (Amis et al., 1981b), and the data acquisition and analysis procedures are also the same.

*Electrophoretic Light Scattering.* The instrument is the same as the one reported earlier from this laboratory (Shaya et al., 1974) except that we now use a spectrum analyzer (Nicolet Scientific, Model 444A) for the frequency domain analysis. The cell design has also been detailed (Caflisch et al., 1980). It consists of two parallel plate platinum electrodes rigidly mounted in slots in a cylinder of KEL-F which fits snugly into a 12-mm polished NMR tube. The electrode spacing ($d$) is 1.84 mm. The pulse generator for the 1-Hz modulation field (Bennett & Uzgiris, 1973) has also been described elsewhere (Caflisch, 1979).

The apparatus was calibrated with bovine serum albumin as the standard (Caflisch et al., 1980). The field-induced Doppler shift frequency ($\Delta\nu_s$) was measured at four or more combinations of $\theta$ and $V_{pp}$ for each solution where the scattering angle ($\theta$) was $6° \leq \theta \leq 9°$, and the peak to peak applied voltage ($V_{pp}$) was $6 \leq V_{pp} \leq 10$ V. The shift frequency $\Delta\nu_s$ is related to the electrophoretic mobility $\mu$ (Ware & Flygare, 1971) by

$$\Delta\nu_s = [n\mu V_{pp}/(\lambda_0 d)] \sin(\theta/2) \cos(\theta/2) \quad (1)$$

$$\Delta\nu_s \approx 10^3 \mu(\theta V_{pp}) \ (\theta \leq 9°, \lambda_0 = 632.8 \text{ nm}) \quad (2a)$$

$$\Delta\nu_s \approx 0.84 \times 10^3 \mu(\theta V_{pp}) \ (\theta \leq 9°, \lambda_0 = 752.5 \text{ nm}) \quad (2b)$$

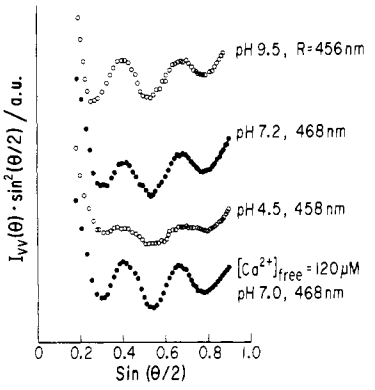


FIGURE 1: Elastic light-scattering profiles of DMV at different pHs without $Ca^{2+}$ and in 120 $\mu$M free $Ca^{2+}$. The DMV radius $R$ is determined from the angular positions of extrema for each profile with the use of the spherical shell model.

where the refractive index ($n$) of water equals 1.332 and the incident wavelength ($\lambda_0$) equals 632.8 (He/Ne laser) or 752.5 nm (Kr ion laser). Thus, eq 2a and 2b give $\mu$ in units of $cm^2$ $V^{-1}$ $s^{-1}$ if $\theta$ is expressed in degrees and $V_{pp}$ in volts.

In order to avoid possible changes in pH of the sample during measurements by electrolysis, we have applied a smaller voltage (6–10 V) for as short a duration as possible than with BSA in our earlier study.

*Potentiometric Titration.* Potentiometric titration of the vesicle suspension was carried out with a pH meter (Beckman Model 3500) calibrated earlier with a set of reference buffer solutions under an argon atmosphere. In conjunction with the DMV number density in a given suspension, the titration result is used to deduce the total charge (titration valency) per DMV. Vesicle suspensions were prepared by adding an appropriate amount of NaCl to those suspensions that were passed through a mixed bed of the ion-exchange resins.

The number of dissociated protons per vesicles ($-r$) as the pH is incremented was deduced under the assumption (Tanford, 1961) that there were negligible electrostatic interactions on the vesicle surface, which seems sensible in view of the surface charge density calculated on this basis (see below).

## Results

*pH Dependence.* In Figure 1, we display some examples of elastic light scattering at different pHs. The vesicle radius ($R$) is calculated from each peak and valley of a scattering profile by assuming the spherical shell structure (Yu, 1982), and the average $R$ so calculated is shown for each profile. At the bottom, we also show a profile in 0.12 mM $Ca^{2+}$. All four profiles give rise to the same set of extrema positions, indicating that the presence of $Ca^{2+}$ does not appear to change the vesicle radius. The complete set of these measurements is collected in Table I. It is quite apparent that the vesicle radius is practically the same regardless of pH in both media, 4 mM imidazole and 2 mM NaCl, and there appears to be only a slight difference in the two media although the difference is not larger than the experimental uncertainty.

Quasi-elastic light-scattering measurements are performed to obtain the translational diffusion coefficient ($D$) of DMV. The autocorrelation function of the scattered photocounts is analyzed by a single exponential function or by the second-order cumulant method (Koppel, 1972) to deduce the decay constant ($\Gamma$); it is in turn proportional to the square of the scattering wave vector ($\mathbf{q}$), and its proportionality constant is $D$. Normally, we measure the scattering at about 10–12 scattering angles whereby the linearity of $\Gamma$ vs. $\mathbf{q}^2$ is confirmed for each set of the $D$ determination. The customary tem-

Table I: Disk Membrane Vesicle Radius by Elastic Light Scattering

| 2 mM NaCl | | 4 mM Im with 20 $\mu$M EGTA | |
|---|---|---|---|
| pH | $R$ (nm)[a] | pH | $R$ (nm)[a] |
| 3.8 | 471 | 3.3 | 454 |
| 4.0 | 471 | 4.1 | 460 |
| 4.1 | 448 | 4.5 | 458 |
| 4.7 | 443 | 5.1 | 457 |
| 5.1 | 454 | 5.7 | 453 |
| 5.5 | 442 | 6.3 | 466 |
| 5.7 | 467 | 7.2 | 468 |
| 5.9 | 459 | 7.8 | 469 |
| 6.0 | 437 | 8.7 | 457 |
| 6.7 | 447 | 9.5 | 456 |
| 7.5 | 439 | | |
| 8.1 | 441 | | |
| 8.4 | 437 | | |
| 9.2 | 441 | | |

[a] Errors in the determination of $R$ are estimated as 1.5–2% from the consistency of extrema positions.

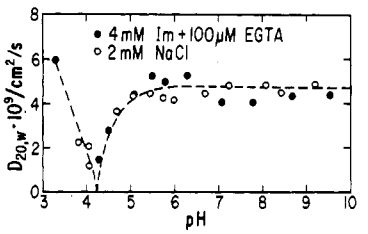


FIGURE 2: Translational diffusion coefficient of DMV ($D_{20,w}$), after correcting for temperature and viscosity, plotted against pH in two different suspending media.

perature and viscosity corrections are applied to represent $D$ at 20 °C in 1 cP viscosity, namely, that of water at the same temperature ($D_{20,w}$). The pH dependence of $D_{20,w}$ is displayed in Figure 2, where the two suspending media, 4 mM Im with 100 $\mu$M EGTA and 2 mM NaCl, have been employed. The dashed curve is drawn to indicate the observed trend. It is obvious from the figure that $D_{20,w}$ is the same in both suspending media over the entire pH range, and further, it is independent of pH above 5 at the asymptote of $4.7 \times 10^{-9}$ $cm^2/s$. Below pH 5, $D_{20,w}$ decreases precipitously and appears to approach a minimum value at about pH 4.3 before it increases again, perhaps beyond the high-pH asymptote. Parenthetically, we should note that there appears to be no such change in the DMV radius with pH by elastic light scattering as shown in Table I; we shall return to this point later, but for now it suffices to postulate that the decrease in $D_{20,w}$ may be due to the intervesicle aggregation induced by low surface charge density whereas it would not affect the radius determination from elastic light-scattering profiles.

Turning to the results of electrophoretic light scattering, we display some typical Doppler-shifted power spectra in Figure 3. A given power spectrum [$S(\nu)$] contains some unshifted component which can arise from the scattering due to the vesicles outside of the electrode space, hence, not under the same uniform electric field and from possible uncharged contaminants. In Figure 3A, we show a progressive decrease in the shift frequency $\Delta\nu_s$ as the pH of the suspending medium is lowered, from 22 Hz at pH 7.9 to 13 Hz at pH 5.5. As is apparent from these spectra, the precision of $\Delta\nu_s$ determination is about 1 Hz. In Figure 3B, a similar trend in $\Delta\nu_s$ is displayed as the free $Ca^{2+}$ concentration is raised under a constant pH. The electrophoretic mobility $\mu$ of DMV is determined from the observed $\Delta\nu_s$ at different $\theta V_{pp}$ values via eq 2a,b, and the

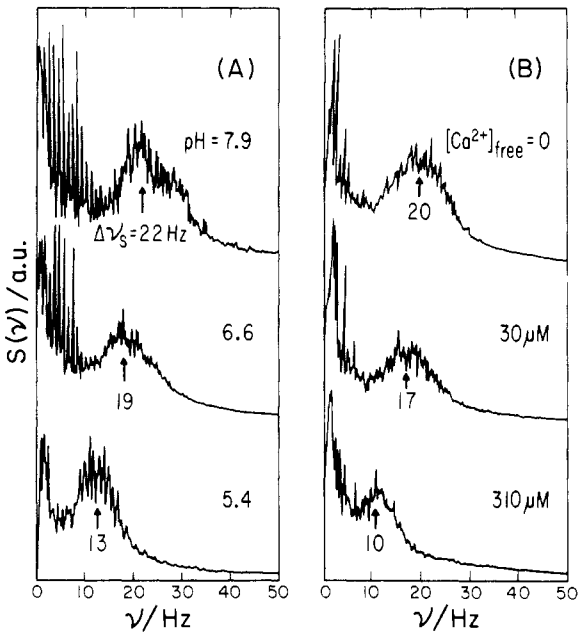


FIGURE 3: Doppler-shifted power spectra $[S(\nu)]$ of electrophoretic light scattering of DMV shown at different pHs (A) and in different free calcium ion concentrations (B). (A) pH dependence of $S(\nu)$ in 4 mM Im + 100 μM EGTA; (B) $[Ca^{2+}]_{free}$ effect on $S(\nu)$ in 4 mM Im + 20 μM EGTA, pH 7.0 ± 0.1. Precision of the shift frequency determination is about 1 Hz in both cases.

customary temperature and viscosity corrections are applied to arrive at $\mu_{20,w}$. The electrophoretic mobility of a charged spherical particle with a diffusion coefficient $D$ and an electrokinetic valency $Z$ suspended in an electrolyte solution having a Debye screening length $\kappa^{-1}$ is

$$\mu = \frac{ZeD}{kT} f(\kappa R) \qquad (3)$$

where $e$ is the elementary charge, $f(\kappa R)$ represents the correction factor for diffuse double-layer screening (Henry, 1931; Tiselius & Svensson, 1940; Alberty, 1948a,b; Wiersema et al., 1966; Shaw, 1969), and $kT$ has the usual meaning. In order to extract the electrokinetic valency $Z$ (or electrokinetic charge $Ze$) from $\mu_{20,w}$, we need to reduce the mobilities at different ionic strengths, i.e., different $\kappa$ values from those at a reference ionic strength. Such a reduction of the mobility is effected by applying small but finite corrections via the diffuse layer screening factor $f(\kappa R)$ such as Henry's theory (Caflisch et al., 1980). Since 4 mM Im at pH 7 has an ionic strength of 2 mM, we choose this as the reference state, and all $\mu_{20,w}$ values are reduced to the values that would be expected if the ionic strength were 2 mM. In so doing, we assume that $Z$ depends only on pH and $D$ does not change with pH for the entire range. The first assumption is entirely reasonable, and the second is justified by noting that the DMV radius does not change much with pH while the observed $D$ (Figure 2) passes through a minimum at pH 4.3, but this is ascribed to the artifact of vesicle aggregations. Thus, $D$ as a measure of the Stokes radius for isolated vesicles should remain constant. The electrophoretic mobility data thus obtained, and reduced, are collected in Table II at different pHs and the corresponding total ionic strengths. The sign of the mobility is assigned on the basis that DMV should be negatively charged at pH 7.

In terms of eq 3, the reduced mobility $\mu_r$ at 2 mM ionic strength at 20 °C in a medium with a viscosity of 1 cP should then be directly proportional to the electrokinetic valency of DMV in a similar medium. In Figure 4, we plot the absolute value of the mobility against pH. The observed (and $T/\eta$ corrected) and reduced values are distinguished by filled and open circles, respectively, when they are perceptibly different. Since the electrophoretic mobility $\mu$ is sensitive only to the surface charge density of $Ze$ (Ware, 1982), we should expect that $\mu$ would not be affected by the aggregation phenomenon which affects $D$ as shown in Figure 2. The results in Figure 4 can therefore be accepted as arising from the charge density decrease as the pH is lowered. Thus, Figure 2 and 4 are two separate manifestations of the isoelectric point and not the identical observation plotted differently. Hence, we have a firm indication that pH 4.3 is the isoelectric point whereby the vesicle aggregation will likely be promoted at this pH as we have seen in Figure 2. To the best of our knowledge, this is the first determination of the isoelectric point of retinal disk membrane, be it in the disk shape or in the vesicular form. We should, however, recall the earliest reported measurement of the isoelectric points of rhodopsin and opsin, 4.5 and 4.6,

Table II: pH Dependence of Electrophoretic Mobility of Disk Membrane Vesicles Suspended in 4 mM Imidazole with 100 μM EGTA

| pH | $I$ (mM)[a] | $\lvert\mu_{20,w}\rvert \times 10^4$ [cm²/(V·s)][b] | $\lvert\mu_r\rvert \times 10^4$ [cm²/(V·s)][c] |
|---|---|---|---|
| 3.8 | 4.3 | 0.8 ± 0.2 | 0.9 ± 0.2 |
| 3.9 | 4.3 | 0.7 | 0.7 |
| 4.0 | 4.3 | 0.7 ± 0.2 | 0.7 ± 0.2 |
| 4.1 | 4.3 | 0.5 | 0.5 |
| 4.2 | 4.2 | 0.5 | 0.5 |
| 4.5 | 4.2 | 1.1 ± 0.5 | 1.2 ± 0.5 |
| 4.7 | 4.2 | 1.0 | 1.1 |
| 5.0 | 4.2 | 1.7 | 1.8 |
| 5.1 | 4.2 | 1.6 | 1.7 |
| 5.2 | 4.2 | 1.6 | 1.7 |
| 5.4 | 4.1 | 2.0 | 2.1 |
| 5.5 | 4.1 | 2.1 | 2.2 |
| 5.7 | 4.1 | 2.2 | 2.3 |
| 5.9 | 3.9 | 2.4 | 2.5 |
| 6.1 | 3.7 | 2.5 | 2.7 |
| 6.5 | 3.3 | 2.9 | 3.1 |
| 6.6 | 3.0 | 3.1 | 3.2 |
| 6.8 | 2.7 | 3.4 | 3.5 |
| 7.1 | 2.0 | 3.5 | 3.5 |
| 7.3 | 1.4 | 3.7 | 3.7 |
| 7.5 | 1.2 | 3.8 | 3.8 |
| 7.9 | 0.6 | 3.9 | 3.9 |
| 8.0 | 0.5 | 3.8 | 3.8 |
| 8.4 | 0.4 | 3.9 | 3.9 |
| 8.8 | 0.5 | 3.8 | 3.8 |
| 8.9 | 0.5 | 4.0 | 4.0 |
| 9.5 | 0.6 | 4.1 | 4.1 |

[a] Total ionic strength of the suspending medium. [b] The temperature- and viscosity-corrected mobility; the error in each is estimated as about ±0.1 unless indicated otherwise. [c] The ionic strength reduced (to 2 mM) mobility; the error in each value is shown similar to that in footnote *b*.

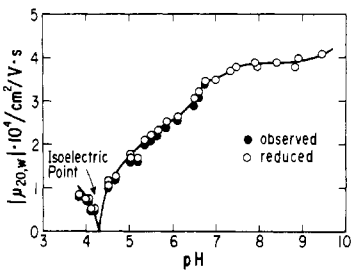


FIGURE 4: pH dependence of the absolute value of electrophoretic mobility. The observed values after being corrected for temperature and viscosity ($|\mu_{20,w}|$) are distinguished from the reduced values, all to 2 mM ionic strength, when the differences are perceptible. The solid curve is drawn merely to indicate the trend of the experimental data.

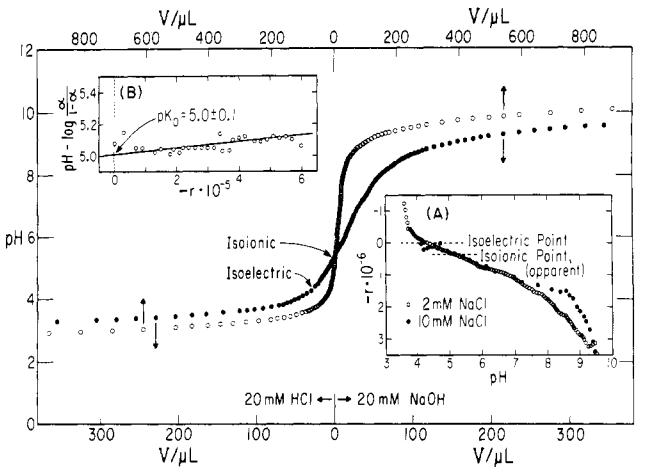


FIGURE 5: Titration curves of an ion-exchanged DMV suspension in 2 mM NaCl (open circles, top abscissa) and of the blank without DMV (filled circles, bottom abscissa). In the inset A, the titration valency of DMV (the number of dissociated protons per vesicle) ($-r$), calculated from the volume of acid or base added and the number density of DMV, is plotted against pH in two different suspending media, 2 and 10 mM NaCl. In the inset B, an intrinsic dissociation constant ($K_0$) determination, attributed to carboxylic acid groups on the DMV surface, is displayed where $pK_0$ is found to be 5.0 ± 0.1.

respectively, of frog retina (Broda & Victor, 1940). It is not surprising, therefore, to find an isoelectric point of 4.3 for DMV because the majority of DMV charge should come from the photopigments. The mobility profile in Figure 4 also shows several dissociation steps beyond pH 4.3 although quantitative determination of the equivalence points may be difficult with the data in Figure 4.

To complement such findings by the electrophoretic mobility of DMV, we have performed potentiometric titrations, and the results are shown in Figure 5. The starting volume of the DMV suspension, after passing through a mixed bed of ion-exchange resins and adding NaCl to make it 2 or 10 mM, was 24 mL and contained $2.8 \times 10^{11}$ vesicles. The bottom abscissa applies to a 2 mM NaCl blank, and the top one to the DMV suspension in 2 mM NaCl. The apparent isoionic point is where we start the titration. We show in the inset A the calculated titration valency per vesicle ($-r$) as a function of pH. It is striking that the two profiles, $-r$ vs. pH and $\mu$ vs. pH (Figure 4), show several dissociation steps at about the same pH regions. Moreover, there seems to be a substantial ionic strength effect on the titration valency profile as seen by the difference in those of 2 and 10 mM NaCl; note, however, that a parallel experiment in the electrophoretic light scattering cannot be performed due to the electrolysis problems with 10 mM NaCl. In the inset B, we display the analysis scheme (Tanford, 1961) to determine an intrinsic dissociation constant ($K_0$), which is attributed to the dissociation of carboxylic groups in the vicinity of pH 5; the reduced charge number $\alpha$ is defined as $(r - r_0)/(r_1 - r_0)$ where $r_1$ and $r_0$ are chosen as $-7.6 \times 10^5$ and $1.2 \times 10^5$ electronic charges, respectively, for the end and beginning points of the carboxylic group dissociation; in other words, the difference between $r_1$ and $r_0$ is the titration valency per vesicle due to the COOH moiety. From the plot in the inset B, we deduce $pK_0 = 5.0 \pm 0.1$ and surmise from the shallow slope of the plot that there exist negligible electrostatic interactions among dissociated carboxylate groups. Since the $pK_0$ of COOH in proteins and polyelectrolytes is around 4.6–4.9 (Tanford, 1961), our assignment of this dissociation step as that due to COOH seems quite reasonable. It is likely that the dissociation step below pH 4 should arise from phosphate groups and that above pH 6 from various types of amino groups though we cannot make definite assignments from the results in Figure 5.

Table III: $Ca^{2+}$ Effect on Electrophoretic Mobility of DMV

| added $[Ca^{2+}]$ ($\mu$M)[a] | added [EGTA] ($\mu$M)[a] | $\lvert\mu_{20,w}\rvert \times 10^4$ [$cm^2/(V \cdot s)$][b] |
|---|---|---|
| Without EGTA Washing Step | | |
| 0 | 0 | 3.3 |
| 20 | 0 | 2.4 |
| 20 | 20 | 2.8 |
| 20 | 100 | 3.3 |
| 20 | 200 | 3.6 |
| With EGTA (100 $\mu$M) Washing Step | | |
| 0 | 100 | 3.6 |
| 5 | 100 | 3.5 |
| 10 | 100 | 3.7 |
| 20 | 100 | 3.7 |
| 30 | 100 | 3.6 |
| 50 | 100 | 3.7 |

[a] Nominal concentrations in the suspending medium (4 mM Im, pH 7.0) adjusted by deliberate additions, not to be confused with the actual concentration. [b] Error range is similar to that in Table II.

*Calcium Ion Binding.* At the start, we show the effect of "endogenous" divalent cations, presumably $Ca^{2+}$, on the observed electrophoretic mobility ($|\mu_{20,w}|$) at pH 7 in 4 mM Im. When DMV suspensions were prepared without specific efforts to remove divalent cations, we observe the values of $|\mu_{20,w}|$ scattered between $2.4 \times 10^{-4}$ and $3.3 \times 10^{-4}$ $cm^2/(V \cdot s)$, and they are usually irreproducible and inconsistent from sample to sample. Upon washing DMV suspensions with 100 $\mu$M EGTA at the end of the preparation procedure and maintaining the EGTA concentration at 100 $\mu$M in the suspending medium, we observe consistently $(3.7 \pm 0.1) \times 10^{-4}$ $cm^2/(V \cdot s)$. With a DMV suspension without the EGTA washing step, the observed electrophoretic mobility is less than $2.7 \times 10^{-4}$ $cm^2/(V \cdot s)$. Subsequent addition of EGTA to the same suspension causes the mobility to first be brought back up to the starting point value and eventually to $(3.7 \pm 0.1) \times 10^{-4}$ $cm^2/(V \cdot s)$ upon further addition. A set of experiments performed to show the possible endogenous $Ca^{2+}$ effect on $\mu_{20,w}$ is collected in Table III. From these observations, we conclude that the exact control of $Ca^{2+}$ concentration is essential in defining the mobility of DMV, and $Ca^{2+}$ must be binding to the DMV surface to reduce its electrophoretic mobility. Hence, one can probe $Ca^{2+}$ binding by this method.

In controlling the concentration of free calcium ion ($C$) in the suspending medium, we make use of calcium ion buffers by appropriately mixing $CaCl_2$ solutions with 20 $\mu$M EGTA solution according to the association equilibrium expressions with the known constants (Potter & Gergely, 1975). The decreasing trend in the electrophoretic mobility with $C$ is shown in Figure 3B where the Doppler-shifted peak position moves toward lower frequency with increasing $C$. We have determined the mobility over 3 logarithmic decades in $C$, 0.5 $\mu$M to 2 mM, and the data were corrected for temperature and viscosity as in the previous case of pH dependence, and the Debye–Hückel screening effect was reduced to that in 2 mM ionic strength as before. The results so obtained are displayed in Figure 6 and collected in Table IV. Here, as in Figure 4, we also distinguish the observed $\mu_{20,w}$ (filled circles) from the reduced $\mu_r$ (open circles) when they are perceptibly different. The ionic strength $I$ of the suspending medium is shown by the dashed curve which spans from 2 to 8 mM for the $C$ range examined. We defer the discussion of the data points represented by (×). The solid curve drawn over the open circles

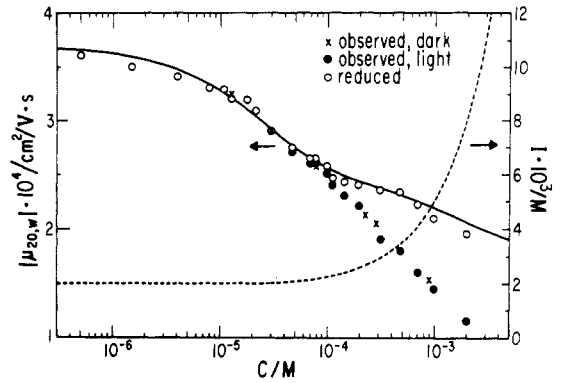


FIGURE 6: Absolute value of electrophoretic mobility corrected for temperature and viscosity ($|\mu_{20,w}|$) of DMV in 4 mM imidazole at pH 7 plotted against the free calcium ion concentration ($C$). The observed values in the unbleached state (measured with a 752.5-nm line of a Kr ion laser as the incident radiation) and in the bleached state (with a 632.8-nm He/Ne laser as the incident source) are distinguished by (×) and (●). The reduced values (○) of the bleached-state data are obtained by applying the ionic strength dependence, all reduced to those in 2 mM ionic strength. The dependence of ionic strength ($I$) on $C$ is shown by the dashed curve. The solid curve represents the analysis result of the binding isotherm according to a model of two independent and noncooperative binding sites.

Table IV: $Ca^{2+}$ Binding Effect on the Electrophoretic Mobility of Bleached-State DMV in 4 mM Imidazole with 20 μM EGTA at pH 7.0 ± 0.1

| $[Ca^{2+}]$ added (μM) | $C$ (μM) | $I$ (mM) | $\lvert\mu_{20,w}\rvert \times 10^4$ [cm²/(V·s)][a] | $\lvert\mu_r\rvert \times 10^4$ [cm²/(V·s)][a] |
|---|---|---|---|---|
| 0 | 0 | 1.9 | 3.7 | 3.7 |
| 17 | 0.5 | 2.0 | 3.6 | 3.6 |
| 20 | 1.5 | 2.0 | 3.5 | 3.5 |
| 23 | 4 | 2.0 | 3.4 | 3.4 |
| 27 | 8 | 2.0 | 3.3 | 3.3 ± 0.2 |
| 30 | 11 | 2.0 | 3.3 | 3.3 |
| 33 | 13 | 2.0 | 3.2 ± 0.2 | 3.2 ± 0.2 |
| 37 | 17 | 2.0 | 3.2 | 3.2 |
| 42 | 22 | 2.0 | 3.1 | 3.1 |
| 50 | 30 | 2.0 | 2.9 | 2.9 |
| 67 | 47 | 2.1 | 2.7 | 2.7 |
| 90 | 70 | 2.2 | 2.7 | 2.7 |
| 100 | 80 | 2.2 | 2.6 | 2.7 |
| 120 | 100 | 2.3 | 2.5 | 2.6 |
| 130 | 110 | 2.3 | 2.4 | 2.5 |
| 170 | 150 | 2.4 | 2.3 | 2.4 |
| 220 | 200 | 2.6 | 2.2 | 2.4 |
| 330 | 310 | 3.0 | 1.9 | 2.4 |
| 500 | 480 | 3.4 | 1.8 | 2.3 |
| 720 | 700 | 4.0 | 1.6 | 2.2 |
| 1020 | 1000 | 5.0 | 1.4 | 2.1 ± 0.2 |
| 2020 | 2000 | 8.0 | 1.1 | 1.9 ± 0.2 |

[a] The error range is the same as that indicated in Table II.

represents the analysis result according to a two binding site model. The data of the reduced mobility show clearly that there are two well-separated steps in decreasing the mobility with increasing $C$, the free $Ca^{2+}$ concentration. As a first approximation, we attempt to analyze the mobility profile with the assumption that there is no ion exchange between added $Ca^{2+}$ and other cations endogenously bound on the DMV surface; this assumption is required because the electrophoretic mobility would not be affected by such an exchange with the valency conservation; e.g., two protons are exchanged for one $Ca^{2+}$. If such an exchange is taking place simultaneously with the net binding, then the profile in Figure 6 should represent only the part due to the net binding on the external surface of DMV. As the starting point, we try a model of independent and noncooperative binding with two different types of binding sites. The appropriate expression for the fraction of binding sites occupied by $Ca^{2+}$ is

$$\frac{r(C)}{n} = \frac{K_1 C}{1 + K_1 C} X + \frac{K_2 C}{1 + K_2 C}(1 - X) \tag{4}$$

where $r(C)$ is the average number of bound $Ca^{2+}$ per DMV, $n$ is the total number of binding sites per DMV, $X$ is the fraction of the high-affinity binding sites, and $K_1$ and $K_2$ are the binding constants for the high-affinity and low-affinity bindings, respectively, i.e., $K_1 > K_2$. Under the assumption of no cation exchange and with the use of eq 3, we can express $r(C)$ and $n$ as

$$r(C) = [1/(2\alpha)][\mu_0 - \mu(C)] \tag{5}$$

$$n = [1/(2\alpha)](\mu_0 - \mu_\infty) \tag{6}$$

with

$$\alpha \equiv [e/(kT)] D_0 f(\kappa_0 R) \tag{7}$$

where the factor of 2 in eq 5 and 6 arises from $Ca^{2+}$ being a divalent cation (hence, each binding reduces $Z$ by 2), $\mu_0$ and $\mu_\infty$ are the mobilities at $C = 0$ and $C = \infty$, respectively, and $D_0$ and $\kappa_0$ in eq 7 are the translational diffusion coefficient and the reciprocal of the Debye screening length, respectively, both at the reference state. Since we define the reference state at 2 mM ionic strength, the corresponding $\kappa_0$ is known, and we have separately determined $D$ and $R$ in different $C$ and established them to be invariant with $C$ for the entire range; the value of $\alpha$ is a known constant. Hence, $r(C)$ can be evaluated from the observed mobility $\mu(C)$ through eq 5. A simpler way to analyze the mobility profile of Figure 6 with the model, however, is to express the experimentally observable $\mu(C)$ in terms of the independent variable $C$ and the model parameters. This is done by combining eq 4–7:

$$\frac{\mu_0 - \mu(C)}{\mu_0 - \mu_\infty} = \frac{K_1 C X}{1 + K_1 C} + \frac{K_2 C (1 - X)}{1 + K_2 C} \tag{8}$$

If we devise a scheme to extrapolate $\mu(C)$ to deduce $\mu_\infty$, then the left-hand side of eq 8 becomes a completely determinable experimental quantity, and the right-hand side contains three adjustable parameters. Recasting eq 8 to facilitate the extrapolation to $C \to \infty$, we have

$$\frac{1}{\mu_0 - \mu(C)} = \frac{1}{\mu_0 - \mu_\infty} + \left(\frac{X}{K_1} + \frac{1 - X}{K_2}\right)\left(\frac{1}{\mu_0 - \mu_\infty}\right)\frac{1}{C} \tag{9}$$

or

$$\frac{\mu_0 - \mu(C)}{C} = \left(\frac{X}{K_1} + \frac{1 - X}{K_2}\right)[\mu(C) - \mu_\infty] \tag{10}$$

These two equations suggest the two ways to extract $\mu_\infty$: (1) from eq 9, the ordinate intercept of the plot $[\mu_0 - \mu(C)]^{-1}$ vs. $C^{-1}$ should give $(\mu_0 - \mu_\infty)^{-1}$, and (2) from eq 10, the abscissa intercept of the plot $[\mu_0 - \mu(C)]/C$ vs. $\mu(C)$ should yield $\mu_\infty$. For the sake of brevity, we will not reproduce these plots here but only state the results deduced from the plots. Both plots yield $\mu_\infty$ as $(1.7 \pm 0.1) \times 10^{-4}$ cm²/(V·s) and also a well-defined break; hence, the hypothetical asymptote corresponding to the high-affinity binding $\mu_b$ is estimated as $(2.4 \pm 0.1) \times 10^{-4}$ cm²/(V·s), which is the expected asymptotic mobility if there were only the high-affinity binding. From the values of $\mu_0$, $\mu_b$, and $\mu_\infty$, we can estimate the fraction of high-affinity binding

$$X = \frac{\mu_0 - \mu_b}{\mu_0 - \mu_\infty} \tag{11}$$

as 0.65 ± 0.10. Having on hand $\mu_\infty$ and $X$, it is now a easy task to deduce $K_1$ and $K_2$ from eq 8. The values are $K_1 = (4.5 \pm 0.8) \times 10^4$ $M^{-1}$ and $K_2 = (4 \pm 2) \times 10^2$ $M^{-1}$. Having established the three adjustable parameters on the right-hand side of eq 8, we finally come to the solid curve in Figure 6 which is drawn according to

$$\mu(C) = \mu_0 - (\mu_0 - \mu_\infty)\left[\frac{K_1 X C}{1 + K_1 C} + \frac{K_2(1 - X)C}{1 + K_2 C}\right] \quad (12)$$

with $\mu_0 = 3.7 \times 10^{-4}$ $cm^2/(V \cdot s)$, $\mu_\infty = 1.7 \times 10^{-4}$ $cm^2/(V \cdot s)$, $K_1 = 4.5 \times 10^4$ $M^{-1}$, $K_2 = 4 \times 10^2$ $M^{-1}$, and $X = 0.65$. Given the reasonable agreement between the solid curve and the data points, it seems fruitless to pursue further refinement of the model.

The data points marked by (×) in Figure 6 are the mobilities of DMV in the unbleached state. We note an excellent agreement between the mobility profile in the bleached state (filled circles) and that in the unbleached state. The data points are obtained by performing the electrophoretic light-scattering experiments with the incident wavelength of 752.5 nm from a krypton ion laser instead of the He/Ne laser output of 632.8 nm used for the bleached-state DMV. As stated under Materials and Methods, we have independently confirmed the preservation of the photochemical state of rhodopsins on DMV after similar exposure to 752.5-nm radiation as in the scattering experiments. Thus, we are assured of the innocuity of the probing radiation relative to the rhodopsin photochemical state; this is to be contrasted to the 632.8-nm output of the 2-mW He/Ne laser which has been shown to damage rhodopsin (Norisuye & Yu, 1977). Within the experimental uncertainty of the mobility determination, we cannot distinguish the two sets of data. If anything, it demonstrates the reproducibility of our experiments with separate retinal samples performed by different experimenters at two separate periods interceded by about 6 months.

*Surface Charge Density.* Combining the results of potentiometric titration with those of the mobility determinations at different pHs and free calcium ion concentrations, we deduce the electrokinetic charge and the number of calcium ion binding sites per DMV as follows. With the radius $R$ by elastic light scattering as 470 nm, we obtain $\kappa_0 R = 68$ in a 2 mM ionic strength medium at 20 °C. Since $\kappa_0 R$ is as large as 68, we can safely use Henry's equation (Henry, 1931) to correct for the diffuse electrical double-layer screening (Wiersema et al., 1966). The correction factor $f(\kappa_0 R)$ in eq 3 is calculated as $2.12 \times 10^{-2}$. With $D_{20,w} = 4.7 \times 10^{-9}$ $cm^2/s$, $\alpha$ defined by eq 7 is then evaluated as $4.5 \times 10^{-9}$ $cm^2/(V \cdot s)$. Given the mobility $\mu_0$ of $3.7 \times 10^{-4}$ $cm^2/(V \cdot s)$ in the absence of $Ca^{2+}$ in 4 mM Im/20 μM EGTA at pH 7, we calculate the electrokinetic valency $Z_0$ at $C = 0$ as $(8.2 \pm 0.3) \times 10^4$ through $\mu_0 = \alpha Z_0$. The titration valency at pH 7 in 2 mM ionic strength on the other hand is $1.1 \times 10^6$ per DMV as shown in Figure 5A. In other words, about 7.5% of the titration valency is electrokinetically active if we assume that the inner surface of DMV is not accessed by the ion-exchange and titration procedures. On the other hand, the titration valency of $1.1 \times 10^6$ per DMV could well be contributed by both sources of a DMV, the interior and exterior surfaces; this is plausible because the DMV is permeable to $H^+$ and $OH^-$ over the full range of pHs examined, 3.3–9.5, as shown by the independence of its size on pH (see Table I). Assuming the ion exchanging of the interior surface and the titration valency to be equally contributed by the inner and outer surfaces, we may estimate that 15% of the outer surface charges are electrokinetically active instead of 7.5%. The fraction of electrokinetic charge may be even larger than 15% if we consider the modeling of DMV as having a smooth spherical surface with a uniform charge density as used in eq 3, which tends to underestimate the electrokinetic charge. Using eq 6, we determine the total number of $Ca^{2+}$ binding sites $n$ as $(2.2 \pm 0.2) \times 10^4$ per DMV, and with $X = 0.65$, we set the high-affinity binding sites $n_1 = nX$ as $1.4 \times 10^4$ and the low-affinity binding sites $n_2 = n(1 - X)$ as $0.8 \times 10^4$. Since the surface area of a DMV is 2.8 $\mu m^2$ or $2.8 \times 10^8$ $Å^2$, the reciprocal surface charge density, namely, the surface area per unit valency, is evaluated as $5 \times 10^2$ $Å^2$/titration valency (assuming the titration is accessing both sides of DMV) and $3.4 \times 10^3$ $Å^2$/electrokinetic valency in the absence of any calcium ion at pH 7. The calcium ion binding can neutralize up to 54% of the electrokinetic charge at pH 7 in 2 mM ionic strength, i.e., $(\mu_0 - \mu_\infty)/\mu_0 = 0.54$; hence, the reciprocal surface charge density varies from $3.4 \times 10^3$ $Å^2$ to $7.4 \times 10^3$ $Å^2$ per electrokinetic charge in the $Ca^{2+}$ binding process. In terms of the customary charge density units, this range is 0.47–0.22 $\mu C/cm^2$. Of course, all these numbers depend crucially on the validity of our model.

## Discussion

We shall first make comparisons with other calcium ion binding studies. From the protein assay in conjunction with the DMV number density determination in a similar medium, we have found in our laboratory (Amis et al., 1981a) that there is $(5.7 \pm 0.5) \times 10^{-15}$ and $(4.5 \pm 0.6) \times 10^{-15}$ g of protein/DMV by the Lowry et al. (1951) and Bradford (1976) methods, respectively. To be consistent with other $Ca^{2+}$ binding studies using the Lowry assay for the membrane proteins, we shall for the time being restrict ourselves to the result of the Lowry protein assay. We can convert $n_1$ and $n_2$ values of the $Ca^{2+}$ binding sites into $n_1 = 4.1$ nmol of $Ca^{2+}$ binding sites/mg of protein and $n_2 = 2.3$ nmol of $Ca^{2+}$ binding sites/mg of protein with the use of $5.7 \times 10^{-15}$ g of protein (Lowry)/DMV. We compare these numbers to the $Ca^{2+}$ binding studies of Hendricks et al. (1977), where they have performed equilibrium dialysis of isolated disk membranes against $^{45}Ca^{2+}$. They have also found a two binding site behavior as in our model. They report $n_1$ (high-affinity binding) = 5 nmol of $Ca^{2+}$ binding sites/mg of protein and $n_2$ (low-affinity binding) = 195 nmol of $Ca^{2+}$ binding sites/mg of protein in four different suspending media. There is a remarkable agreement in $n_1$ despite the disparity in the techniques adopted. We count the $Ca^{2+}$ binding sites through the observed decrease in the electrokinetic charge of a DMV while they count the same through the membrane-bound $^{45}Ca^{2+}$ regardless of its location of binding, be it inside and/or outside. If the agreement is not due to some fortuitous circumstances, then our assumption of no cation exchange has been validated, and the binding is purely on the outside surface. We should note here that our method is indirect compared to the equilibrium dialysis of radioactive $^{45}Ca^{2+}$ insofar as the $Ca^{2+}$ binding is concerned, but once the agreement is established, our method provides information about the nature of binding whereas the other method can scarcely make reference to the same information. The discrepancy of $n_2$ values between 2.3 nmol of $Ca^{2+}$ vs. their 195 nmol of $Ca^{2+}$ per mg of protein may indeed be due to the process of cation exchange taking place particularly in low-affinity binding. Cation exchange attending the $Ca^{2+}$ binding should not affect the bound calcium counting by their method whereas it gives rise to no change in the electrophoretic mobility; hence, our method is incapable of detecting any binding. We suggest that the difference of nearly 2 orders of magnitude in the $n_2$ value may be due to such a phenomenon as cation exchange. It is also possible, however,

that the difference could be due to $Ca^{2+}$ transport into the intravesicular volume at a high $Ca^{2+}$ concentration gradient across the bilayer. On the basis of our observations alone, we cannot rule out the latter possibility; however, massive transport is unlikely in the millimolar range since DMV have been shown to undergo osmotic deformation in this concentration range (Amis et al., 1981b), indicating that a finite osmolarity gradient is sustained. Hence, the concentration of $Ca^{2+}$ would be different in the suspending medium and interior volume. If we can rule out the $Ca^{2+}$ influx, then the cation exchange mechanism for the low-affinity binding seems a probable cause for the discrepancy in $n_2$. Hendricks et al. have also proposed that the low-affinity binding should be ascribed to nonspecific bindings of $Ca^{2+}$ to the polar heads of phospholipid molecules. In such a case, cation exchange on the phosphate group of the polar heads appears eminently plausible as a similar exchange is well established in nucleic acids (Bleam et al., 1980).

With regard to the surface charge density and related quantities, first of all, 0.47 $\mu C/cm^2$ for the electrokinetic charge in the absence of $Ca^{2+}$ in 2 mM ionic strength at pH 7 is a reasonable number, as in similarly sized polymer latex particles (Bagchi et al., 1979). Second, it is interesting to compare our 1.2 electrokinetic charges/rhodopsin [$8.2 \times 10^4$ electrokinetic charges/DMV and $7 \times 10^4$ rhodopsins/DMV from Amis et al. (1981a)] to the 1.5 electronic charges/rhodopsin on the intradiskal surface deduced by Schnetkamp et al. (1981). Third, we can calculate unambiguously the $\zeta$ potential directly from the electrophoretic mobility with the use of the Helmholtz–Smoluchowski equation because $\kappa_0 R$ exceeds at least 50 (Wiersema et al., 1966). The $\zeta$ potential so calculated is 52 mV, which is to be compared with the "interfacial potential" of −52 mV inferred by Schnetkamp et al. (1981) through the Guoy–Chapman equation on the basis of the observed difference in pH on the membrane surface and that in bulk solution. Whether this agreement is fortuitous remains to be tested. Note that there must be a Stern layer on the DMV surface since the titration valency and electrokinetic valency are substantially different, i.e., $1.6 \times 10^6$ per DMV vs. $8.2 \times 10^4$ per DMV. In such a case, the Guoy–Chapman equation is controlled by the Stern potential, $\Psi_\delta$ (Davies & Rideal, 1963), and only if the Stern plane is close enough to the electrokinetic shear surface for a weakly charged plane can one equate $\Psi_\delta$ to the $\zeta$ potential (Adamson, 1976). If their interfacial potential of −52 mV relative to the bulk solution is indeed $\Psi_\delta$, then the agreement seems more plausible. It is not clear, however, what is meant by the interfacial potential other than taking the entire membrane surface as a distinct continuum, separate from the bulk solution.

Having thus established that the electrophoretic mobility measurements lead to the surface charge characterization and $Ca^{2+}$ binding isotherm of DMV, we next discuss the effect of the photochemical state of rhodopsin. Simply stated, there is no difference in the electrokinetic charge, $\zeta$ potential, and binding behavior between the bleached and unbleached DMV in 4 mM Im at pH 7. This is a remarkable finding. It means that the electrostatic characteristics of the exterior surface of DMV are invariant to photoinduced change in rhodopsin molecules, at least in the suspending media we have tested. It may be well argued that upon removal of the peripheral proteins (G protein and phosphodiesterase) from the disk surface by suspending the disks in low ionic strength media, we have unwittingly rendered the surface of DMV photochemically insensitive. Thus, what we find with the DMV bears no relation to the in vivo photosensitivity of the $Ca^{2+}$ binding of the disks. Alternatively, the photochemical changes might involve the interior surface as suggested by Kaupp et al. (1979, 1980, 1981). If we take our $n_1$ value of $1.4 \times 10^4$, we get 0.2 bound $Ca^{2+}$ per rhodopsin on the exterior surface of DMV in the high-affinity regime, which is to be compared with 0.1–0.2 $Ca^{2+}$ per rhodopsin quoted by Liebman (1974) and Szuts & Cone (1977) for the endogenous $Ca^{2+}$ in ROS. On the other hand, Kaupp et al. (1981) have established that there exist two different calcium pools, one on the interior surface and the other on the exterior surface. Clearly, the issue needs to be settled relative to the findings of Kaupp et al. We emphasize here that our finding of the insignificant effect of bleaching with regard to the electrokinetic charge and calcium binding is a direct observation not dependent on any model or assumption, and our electrostatic and electrokinetic characterizations of DMV are through well-established methods in colloid science. On the other hand, our detailed quantitative descriptions depend on a set of assumptions and stipulations. We list them here for the sake of completeness:

(1) The membrane vesicles move like charged rigid spheres under the applied electric field. (2) The membrane vesicle surface as a whole is negatively charged at pH 7. (3) There exists no cation exchange attendant on $Ca^{2+}$ binding, at least in the high-affinity binding regime. (4) Independent of any endogenous and prebound $Ca^{2+}$, we probe only the binding by exogenous $Ca^{2+}$.

Acknowledgments

A brief but fruitful conversation with Professor Benjamin Chu some years ago is gratefully recalled. We thank our former colleagues, Drs. Hideo Takezoe and Takashi Norisuye, for their advice and comments.

**Registry No.** Ca, 7440-70-2.

References

Adamson, A. W. (1976) *Physical Chemistry of Surfaces*, 3rd ed., Wiley, New York.
Alberty, R. A. (1948a) *J. Chem. Educ. 25*, 426–433.
Alberty, R. A. (1948b) *J. Chem. Educ. 25*, 619–625.
Amis, E. J., Davenport, D. A., & Yu, H. (1981a) *Anal. Biochem. 114*, 85–91.
Amis, E. J., Wendt, D. J., Erickson, E. D., & Yu, H. (1981b) *Biochim. Biophys. Acta 664*, 201–210.
Bagchi, P., Gray, B. V., & Birnbaum, S. M. (1979) *J. Colloid Interface Sci. 69*, 502–528.
Baylor, D. A., & Fourtes, M. G. F. (1970) *J. Physiol. (London) 207*, 77–92.
Bennett, A. J., & Uzgiris, E. E. (1973) *Phys. Rev. A 8*, 2662–2669.
Bleam, M. L., Anderson, C. F., & Record, M. T., Jr. (1980) *Proc. Natl. Acad. Sci. U.S.A. 72*, 3085–3089.
Bradford, M. (1976) *Anal. Biochem. 72*, 248–254.
Broda, E. E., & Victor, E. (1940) *Biochem. J. 34*, 1501–1506.
Caflisch, G. B. (1979) Ph.D. Thesis, University of Wisconsin—Madison, Madison, WI.
Caflisch, G. B., Norisuye, T., & Yu, H. (1980) *J. Colloid Interface Sci. 76*, 174–181.
Davies, J. T., & Rideal, E. K. (1963) *Interfacial Phenomena*, Chapter 3, Academic Press, New York.
Haas, D. D., & Ware, B. R. (1976) *Anal. Biochem. 74*, 175–188.
Hagins, W. A. (1972) *Annu. Rev. Biophys. Bioeng. 1*, 131–158.
Hagins, W. A., & Yoshikami, S. (1974) *Exp. Eye Res. 18*, 299–305.
Hemminki, K. (1975) *Vision Res. 15*, 69–72.

Hendricks, Th., van Haard, P. M. M., Daemen, F. J. M., & Bonting, S. L. (1977) *Biochim. Biophys. Acta 467*, 175–184.
Henry, D. C. (1931) *Proc. R. Soc. London, Ser. A 133*, 106–129.
Josefowicz, J., & Hallet, F. R. (1975) *Appl. Opt. 14*, 740–742.
Kaupp, U. B., Schnetkamp, P. P. M., & Junge, W. (1979) *Biochim. Biophys. Acta 552*, 390–403.
Kaupp, U. B., Schnetkamp, P. P. M., & Junge, W. (1980) *Nature (London) 286*, 638–640.
Kaupp, U. B., Schnetkamp, P. P. M., & Junge, W. (1981) *Biochemistry 20*, 5500–5516.
Koppel, D. E. (1972) *J. Chem. Phys. 57*, 4814–4820.
Liebman, P. A. (1974) *Invest. Ophthalmol. 13*, 700–701.
Lowry, O. H., Rosebrough, N. J., Farr, A. L., & Randall, R. J. (1951) *J. Biol. Chem. 193*, 265–275.
Mohan, R., Steiner, R., & Kaufman, R. (1976) *Anal. Biochem. 79*, 506–525.
Montal, M., Darszon, A., & Trissl, H. W. (1977) *Nature (London) 267*, 221–225.
Norisuye, T., & Yu, H. (1977) *Biochim. Biophys. Acta 471*, 436–452.
Norisuye, T., Hoffman, W. F., & Yu, H. (1976) *Biochemistry 15*, 5678–5682.
O'Brien, D. F. (1979) *Photochem. Photobiol. 29*, 679–685.
O'Brien, D. F., Costa, L. F., & Ott, R. A. (1977) *Biochemistry 16*, 1295–1303.
Potter, J. D., & Gergely, J. (1975) *J. Biol. Chem. 250*, 4628–4633.
Schnetkamp, P. P. M., Kaupp, U. B., & Junge, W. (1981) *Biochim. Biophys. Acta 642*, 213–230.
Shaw, D. J. (1969) *Electrophoresis*, Academic Press, New York.
Shaya, S. A., Han, C. C., & Yu, H. (1974) *Rev. Sci. Instrum. 45*, 280–285.
Smith, H. G., Jr., & Bauer, P. J. (1979) *Biochemistry 18*, 5067–5073.
Smith, H. G., Jr., & Litman, B. J. (1982) *Methods Enzymol. 81*, 57–61.
Smith, H. G., Jr., Stubbs, G. W., & Litman, B. J. (1975) *Exp. Eye Res. 20*, 211–217.
Smith, H. G., Jr., Fager, R. S., & Litman, B. J. (1977) *Biochemistry 16*, 1399–1405.
Szuts, E. Z. (1980) *J. Gen. Physiol. 76*, 253–258.
Szuts, E. Z., & Cone, R. A. (1977) *Biochim. Biophys. Acta 468*, 194–208.
Tanford, C. (1961) *Physical Chemistry of Macromolecules*, Chapter 8, Wiley, New York.
Tiselius, A., & Svensson, H. (1940) *Trans. Faraday Soc. 36*, 16–22.
Tyminski, P. N., Klingbiel, R. T., Ott, R. A., & O'Brien, D. F. (1982) *Biochemistry 21*, 1197–1204.
Uzgiris, E. E. (1974) *Rev. Sci. Instrum. 45*, 74–80.
Uzgiris, E. E., & Kaplan, J. H. (1974) *Rev. Sci. Instrum. 45*, 120–121.
Wald, G. (1968) *Science (Washington, D.C.) 162*, 230–239.
Ware, B. R. (1982) in *Biomedical Applications of Laser Light Scattering* (Sattelle, D. B., Lee, W. I., & Ware, B. R., Eds.) p 293, Elsevier Biomedical Press, Amsterdam.
Ware, B. R., & Flygare, W. H. (1971) *Chem. Phys. Lett. 12*, 81–85.
Wiersema, P. H., Loeb, A. L., & Overbeek, J. Th. G. (1966) *J. Colloid Interface Sci. 22*, 78–99.
Yoshikami, S., & Hagins, W. A. (1971) *Biophys. J. 11*, 47a.
Yu, H. (1982) *Methods Enzymol. 81*, 616–629.